

## Charge Transport in the Diatomic Molecular Solids and Liquids: N<sub>2</sub>, O<sub>2</sub>, and CO

R. J. Loveland, P. G. Le Comber, and W. E. Spear

*Carnegie Laboratory of Physics, University of Dundee, Dundee, Scotland*

(Received 10 February 1972)

The paper reports an investigation of the drift mobility of electronic charge carriers in several phases of the diatomic solids N<sub>2</sub>, O<sub>2</sub>, and CO. It also includes similar measurements on positive and negative ions in the corresponding liquids. Thin crystal specimens (20–400 μm thick) were grown from the liquid between parallel electrodes in a chamber attached to a miniature cryostat after careful purification of the starting gas. As in previous work on the rare-gas solids and liquids, an electron-beam technique was used for the generation of excess carriers near one of the electrodes. Measurement of the transit time led directly to the drift mobility  $\mu$ . In  $\alpha$ - and  $\beta$ -N<sub>2</sub>,  $\beta$ -O<sub>2</sub>, and  $\beta$ -CO electron mobilities between 10<sup>-3</sup> and 10<sup>-2</sup> cm<sup>2</sup> sec<sup>-1</sup> V<sup>-1</sup> were obtained; a similar value was found for the hole mobility in  $\gamma$ -O<sub>2</sub>. The temperature dependence of  $\mu$  has been analyzed in terms of the nonadiabatic small-polaron theory. It is found that low-energy phonons (<10 meV) are involved in the hopping transport. The implications of these results are discussed. In the liquids, Walden's rule is obeyed. With small electrode spacings, the observed transit signals suggest the existence of two mobile species.

### I. INTRODUCTION

The condensed phases of nitrogen, oxygen, and carbon monoxide have received a considerable amount of attention, and crystal structures, lattice dynamics, and many of their basic physical properties have been investigated in some detail. An interesting feature of these diatomic materials is the existence of more than one solid phase. X-ray studies as well as specific-heat and thermal-expansion measurements<sup>1</sup> show that this probably results from the orientational disordering of the molecules in the crystals above a critical temperature. In nitrogen, for example, the  $\alpha$  phase exists up to 35.6 K (space group  $P2_13$ )<sup>2</sup> and the diatomic molecules execute small librations about their center of mass. At 35.6 K, transition to the  $\beta$  phase takes place (space group  $P6_3/mmc$ )<sup>3</sup> in which the molecules are known to precess at an angle of 57° with respect to the  $c$  axis of the crystal.<sup>4</sup>

Carbon monoxide is isomorphous with nitrogen and the  $\alpha$ - $\beta$  transition occurs at 61.6 K. In solid oxygen, three phases have been identified. For the  $\gamma$  phase, the highest-temperature phase, x-ray studies<sup>5</sup> have shown that each of the eight molecules in the unit cell undergoes some form of rotation. Barrett and Meyer<sup>6</sup> proposed that in  $\beta$ -O<sub>2</sub> the molecules precess around the threefold axis, but Raman studies<sup>7</sup> suggest that the  $\beta$  phase may be more akin to the  $\alpha$  phase with its nonrotating molecules.

Nothing is known about the electrical transport properties of the solid phases of N<sub>2</sub>, O<sub>2</sub>, and CO. It seemed, therefore, of some interest to extend our recent studies of the rare-gas solids<sup>8,9</sup> to

diatomic molecular solids. The previous work showed that crystals of Ar, Kr, and Xe possessed remarkable transport properties; the electron mobilities were found to be comparable to those in wide-band semiconductors. For instance in Xe, values about 4000 cm<sup>2</sup> sec<sup>-1</sup> V<sup>-1</sup> have been obtained at 157 K near the triple point. Because of the weak acoustic scattering, hot-electron effects play a predominant part, even at fields below 100 V cm<sup>-1</sup> (in Kr and Xe). The mechanism of hole transport is basically different. The hole mobility in Xe<sup>10</sup> is about  $2 \times 10^{-2}$  cm<sup>2</sup> sec<sup>-1</sup> V<sup>-1</sup> and recent measurements have led to similar values for the other rare-gas solids.<sup>11</sup> The hole results have been interpreted in terms of a phonon-assisted hopping mechanism in which the hole is likely to be localized on a center such as Xe<sub>2</sub><sup>+</sup>.

The present investigation was prompted essentially by the following questions: What is the mechanism of charge transport in typical diatomic molecular solids? How do their transport properties compare with those of the rare-gas solids? To what extent do phase changes and precessional molecular modes affect the carrier mobilities? In the following we attempt to answer some of these questions.

The transport experiments have also been extended into the liquid phase. No electronic component could be detected in charge transport through the above diatomic liquids; in this respect they differ basically from liquid Ar, Kr, and Xe.<sup>8</sup> Results for the positive- and negative-ion mobilities and their temperature dependence are presented in Sec. IV.

## II. EXPERIMENTAL METHOD

The experimental approach used in this work is similar to that described previously in connection with the rare-gas solids and liquids. Only a brief outline will be given here with particular reference to the new features of the redesigned system.

Figure 1(a) is a schematic diagram of the apparatus. The specimen *S* is contained in a small chamber which is cooled by a miniature two-stage cryostat.<sup>12</sup> The specimen chamber, surrounded by a cooled radiation shield *R*, is mounted in the vacuum enclosure *V* in which a pressure of less than  $10^{-5}$  Torr is maintained. Specimens are prepared from the ultra-pure gas<sup>13</sup> contained in the flask *F*. To obtain sufficiently long carrier lifetimes, it was essential to purify further the starting materials. All gases were passed through the carefully outgassed and cooled charcoal trap *C*. In some cases the gettering purification in chamber *G* was used as a second stage. The gas was exposed for about 15 min to the nonevaporable gettering alloy<sup>14</sup> maintained at 400°C. Although the getter was saturated for the gas under investigation, it still was effective in removing impurities.

After purification the gas was condensed into the specimen chamber, the lowest part of which is shown in Fig. 1(b). The first filling was normally pumped away after a few minutes to reduce the residual impurity concentration in the cham-

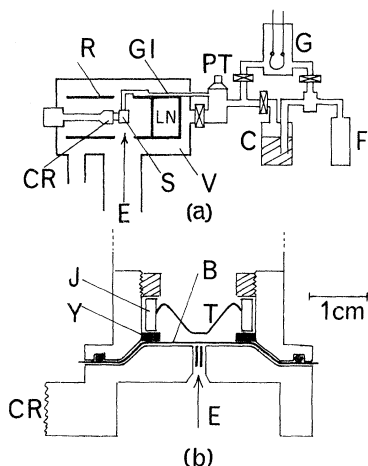


FIG. 1. Experimental arrangement. (a) Schematic diagram of the complete apparatus: C, charcoal trap; CR, cryotip; E, electron beam; F, flask containing starting gas of research-grade purity; GI, gas inlet; G, gettering chamber; PT, pressure transducer; R, liquid-nitrogen (LN) radiation shield; S, specimen chamber; V, vacuum chamber. (b) Details of the specimen chamber (S above): B, coated Mylar top electrode; CR, cryotip; E, electron beam; J, copper ring; T, flexible top electrode; Y, ceramic spacing ring.

ber. The bottom electrode B consisted of an aluminum- or gold-plated Mylar foil ( $12\ \mu\text{m}$  thick) stretched tightly over the lower part of the chamber and held in position by low-temperature varnish and the In O-ring. In experiments on the solids, a flexible top electrode T had to be used. It consisted of a thin wire, flattened at the lower part to cover approximately the area of the fine holes in the copper base through which the electron beam entered. The wire electrode was soldered on to the copper ring J, which was pressed against the spacer Y. In this way electrode spacings in the range between 20 and  $100\ \mu\text{m}$  could be obtained, which proved to be essential in experiments on the solids.

Crystals were grown from the liquid at temperatures and pressures corresponding to the triple point. They measured about 1 cm across and were of sufficient height to include the complete wire electrode. The crystals were examined optically in reflected light and found to be of good quality, but tended to develop cracks when cooled to temperatures below the triple point. However, as a crystal area of only  $10\ \text{mm}^2$  was involved in the experiments, it was generally found that carrier transits in the temperature range of interest were unaffected by cracking.

Electron-hole pairs were generated near the lower electrode by electron beam excitation using pulses between 10- and 300-nsec duration and energies up to 45 keV. The electrons entered the chamber through the Mylar foil with negligible loss of energy. Carriers of one sign were extracted by a synchronized field pulse and their transit time  $t_t$  across the specimen was measured directly on a fast oscilloscope after suitable preamplification. The experimental method has been discussed in more detail in previous publications.<sup>8,15</sup> In the present work  $t_t$  was generally determined by displaying the current signal. Figure 2(a) shows a typical electron transit pulse in solid  $\text{N}_2$  traced from an oscilloscope photograph. Pulses generally had a long diffusive "tail" and the most consistent results were obtained by defining the transit time as  $t_t = \frac{1}{2}(t_1 + t_2)$ . The mobility was deduced from a graph of  $1/t_t$  vs applied potential. It was also found essential to use a space-charge neutralization technique in which only every fourth (or eighth) excitation pulse was accompanied by a field pulse. In this way, each electron transit was preceded by three (or seven) space-charge neutralization pulses, considerably reducing polarization effects due to trapping.

## III. EXPERIMENTAL RESULTS IN THE SOLID PHASES

### A. Nitrogen

Electrons were found to be mobile in both the  $\alpha$  and  $\beta$  phases of nitrogen. No signals that could

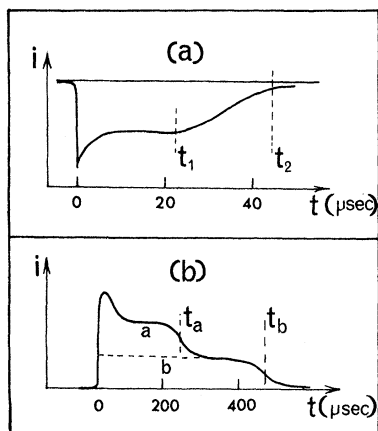


FIG. 2. Observed pulse shapes. (a) Electron-transit pulse in solid nitrogen. The transit time is defined as  $\frac{1}{2}(t_1 + t_2)$ . (b) Positive ion transit in liquid nitrogen ( $d \lesssim 30 \mu\text{m}$ ) suggesting the drift of two species *a* and *b*.

be associated with the transit of holes were detected in either phase. Figure 3 shows the temperature dependence of the electron mobility  $\mu_e$  for a number of crystals between 63 K, the triple point, and 30 K.  $\mu_e$  is plotted logarithmically against  $1/T$ . Between 63 and 52 K, the electron mobility remained approximately constant at  $1.7 \times 10^{-3} \text{ cm}^2 \text{ sec}^{-1} \text{ V}^{-1}$ , but then decreased towards the  $\alpha$ - $\beta$  transition temperature. At this point the signal height dropped and faster electron signals appeared. The first effect indicated a decrease in the generation efficiency of electrons which could have resulted from trapping centers introduced by the large thermal strain at the  $\alpha$ - $\beta$  transition.<sup>1</sup> Although fairly well-defined transits were observed in the  $\beta$  phase, the results shown in Fig. 3 are insufficient to lead to the temperature dependence.

It should be emphasized that in nitrogen, as in the other diatomic solids, the measured drift velocity was always proportional to the applied field up to the highest values used in the experiments ( $E \approx 10^5 \text{ V cm}^{-1}$ ). Because of the low carrier mobilities found here, the hot-electron effects prominent in the rare-gas solids are very unlikely to occur in diatomic solids.

After purification of the gas, electron lifetimes with respect to deep traps were found to lie between 50 and 100  $\mu\text{sec}$  in both phases of solid nitrogen. As fields in excess of  $10^5 \text{ V cm}^{-1}$  could not be used in the specimen chamber, the carrier lifetime set an upper limit of about 100  $\mu\text{m}$  for the specimen thickness. This requirement, together with the need for some degree of flexibility in the top electrode presented a considerable experimental problem. The wire electrode shown in Fig.

1(b) was found to be the most satisfactory solution. It introduced, however, two difficulties. First, it undoubtedly caused some field inhomogeneity which could distort the transit signal. A series of subsidiary experiments in the liquid phase, comparing wire-electrode measurements with results from a rigid-disc electrode, convinced us that this had a negligible effect on the mobility determination.

A more serious problem was the uncertainty in the electrode spacing. Before assembly the surface of the wire electrode was set accurately in the lower plane of the mounting ring. The positive ion mobility in the liquid was found in all the experiments to be a highly reproducible quantity. We used its value at the triple point to determine the electrode spacing  $d$ , both before and after measurements on the crystals. The two values of  $d$  were generally in good agreement. However, the analysis of the results for some thirty crystals showed clearly that during crystal growth a change in the electrode spacing (about  $\pm 5 \mu\text{m}$  or less) must have occurred. An average value of  $1.7 \pm 0.8 \times 10^{-3} \text{ cm}^2 \text{ sec}^{-1} \text{ V}^{-1}$  at 63 K was deduced from these results and the temperature runs in Fig. 3 were normalized to this value. The wide error limits are mainly caused by the uncertainty in  $d$ ; the relative accuracy in the temperature dependence of  $\mu_e$  is within 10%.

### B. Oxygen

The  $\gamma$  and  $\beta$  phases of oxygen were investigated in this work. Holes were mobile in both these phases and Fig. 4 shows the temperature dependence of the hole mobility  $\mu_h$  in the  $\gamma$  phase for several crystals. In the  $\beta$  phase the hole transits were lifetime limited, but indicated a hole mobility

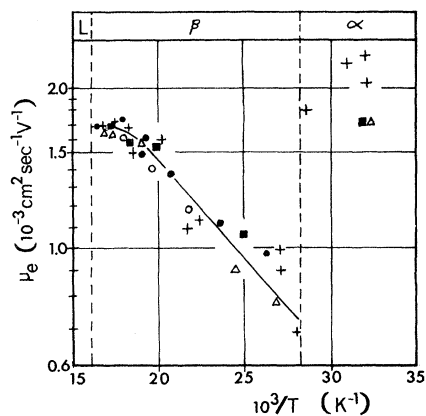


FIG. 3. Electron drift mobility in the  $\beta$  and  $\alpha$  phases of solid nitrogen as a function of the inverse temperature. The symbols refer to different specimens, between 30 and 100  $\mu\text{m}$  thick.

of less than  $10^{-3} \text{ cm}^2 \text{ sec}^{-1} \text{ V}^{-1}$ .

Electrons appeared to be mobile only in the  $\beta$  phase. At the transition temperature (43.8 K),  $\mu_e$  values between  $6 \times 10^{-3}$  and  $10 \times 10^{-3} \text{ cm}^2 \text{ sec}^{-1} \text{ V}^{-1}$  were obtained. Unfortunately, thermal strain caused the signals to decrease rapidly with time after the formation of the  $\beta$  phase and no meaningful conclusions as to the temperature dependence of  $\mu_e$  could be drawn from the results in Fig. 4.

### C. Carbon Monoxide

A preliminary examination has been made of this material. The only definite information obtained so far is that electrons have a mobility of between 2 and  $4 \times 10^{-3} \text{ cm}^2 \text{ sec}^{-1} \text{ V}^{-1}$  at the triple point temperature (68 K).

Table I summarizes the carrier mobilities in solid  $\text{N}_2$ ,  $\text{O}_2$ , and CO at the indicated phase transition temperatures.

## IV. EXPERIMENTAL RESULTS FOR THE LIQUIDS

In all three molecular liquids the temperature dependence of the mobilities of positive and negative carriers was measured at the saturation vapor pressure. The results for  $\text{N}_2$ ,  $\text{O}_2$ , and CO are shown in Figs. 5–7, respectively. In the upper part of Fig. 5 the product  $\mu_+ \eta$ , where  $\eta$  denotes the viscosity,<sup>16</sup> is plotted against  $T$ . Within experimental error,  $\mu_+ \eta$  is independent of temperature, and similar results have been found for  $\text{O}_2$  and CO. Walden's rule is thus obeyed, and supports the interpretation in terms of an ionic transport.

Most of the above measurements were made with electrode spacings greater than 50  $\mu\text{m}$ . When  $d$  was reduced to 30  $\mu\text{m}$  or less, interesting double transit pulses for both positive and negative ions

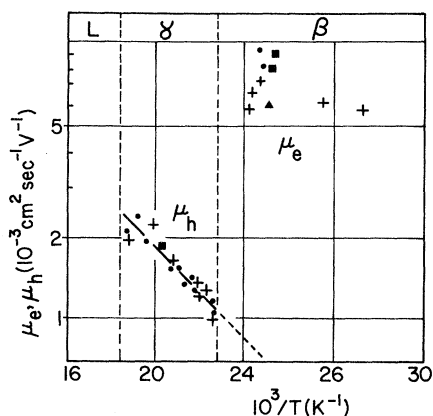


FIG. 4. Hole mobility in  $\gamma$  oxygen and electron mobility in  $\beta$  oxygen plotted as a function of the inverse temperature. The symbols refer to different specimens, between 25 and 50  $\mu\text{m}$  thick.

TABLE I. Electron and hole mobilities for solid nitrogen, oxygen, and carbon monoxide at the indicated phase-transition temperatures.

	Phase	$T$ (K)	Electron mobility ( $\text{cm}^2 \text{ sec}^{-1} \text{ V}^{-1}$ )	Hole mobility ( $\text{cm}^2 \text{ sec}^{-1} \text{ V}^{-1}$ )
$\text{N}_2$	$\beta$	63	$1.7 \times 10^{-3}$	...
	$\alpha$	35	$\sim 2 \times 10^{-3}$	...
$\text{O}_2$	$\gamma$	54	...	$2.3 \times 10^{-3}$
	$\beta$	43	$\sim 8 \times 10^{-3}$	$\sim 10^{-3}$
CO	$\beta$	68	$3 \times 10^{-3}$	...

were observed in  $\text{N}_2$  and  $\text{O}_2$ . Figure 2(b) shows an example. It appears that two species  $a$  and  $b$  are now mobile, defining transit times  $t_a$  and  $t_b$  such that  $t_b/t_a \approx 2$ . Further work in this direction is in progress.

In contrast to the results of Henson<sup>17</sup> and Bruschi *et al.*<sup>18</sup> we did not find any conclusive evidence for steplike discontinuities in mobility with applied field. If the latter exist, our negative result could be due to several reasons. First, the time scale is very different in the two experimental techniques. In the shutter method used by the above authors, ionic transit times were about two orders of magnitude longer than in our experiments. It is likely that longer transit times would enhance the probability of cluster formation or allow the buildup of liquid motion.<sup>19</sup> Another possibly significant difference is in the magnitude of the applied fields:  $6 \times 10^3$  to  $10^5 \text{ V cm}^{-1}$  in our ex-

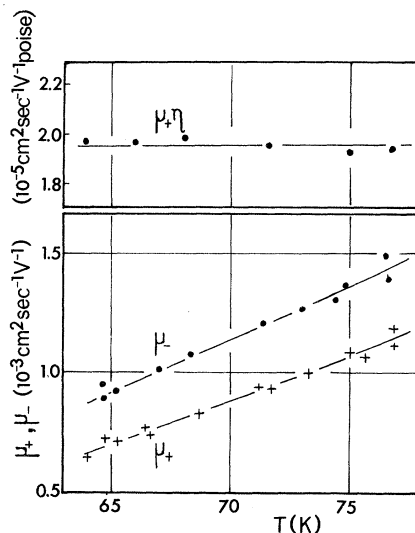


FIG. 5. Temperature dependence of the positive and negative ion mobilities  $\mu_+$  and  $\mu_-$  in liquid nitrogen. Also shown is the temperature dependence of  $\mu_+ \eta$ , where  $\eta$  denotes the viscosity.

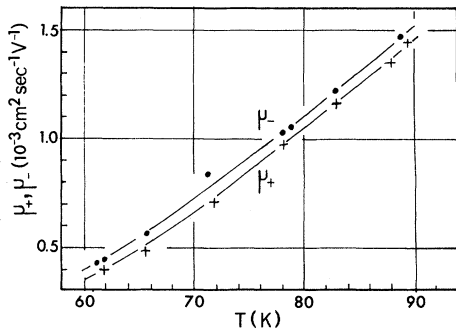


FIG. 6. Temperature dependence of the positive and negative ion mobilities in liquid oxygen.

periments, and  $1 \times 10^2$  to  $4 \times 10^3$   $\text{V cm}^{-1}$  in the shutter method.

### V. DISCUSSION

The results of the present investigation show that carrier mobilities in the diatomic solids lie between  $10^{-3}$  and  $10^{-2}$   $\text{cm}^2 \text{sec}^{-1} \text{V}^{-1}$ . The electronic transport mechanism is therefore basically different from that in the conduction band of the rare-gas solids, whose high electron mobilities appear to be quite exceptional for molecular solids. Evidently, localization of the excess charge carrier plays a predominant part in the diatomic solids. In this respect their transport properties are comparable with the hole conduction in the rare-gas solids<sup>10,11</sup> or with the electron transport in orthorhombic sulphur.<sup>20</sup> It suggests that an interpretation of the results within the framework of small-polaron theory would be a reasonable approach. In this theory, developed by Holstein<sup>21</sup> and others,<sup>22</sup> the localization of the charge-carrier results from the vibrational interaction and transport occurs through phonon-assisted intermolecular hopping.

In the following an attempt has been made to fit the experimental results for  $\beta\text{-N}_2$  and  $\gamma\text{-O}_2$  to the nonadiabatic small-polaron theory; other pos-

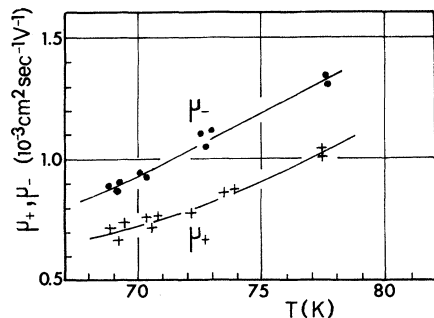


FIG. 7. Temperature dependence of the positive and negative ion mobilities in liquid carbon monoxide.

sibilities will be discussed later. Holstein<sup>21</sup> gives the following expression for the hopping mobility:

$$\mu = \frac{ea^2}{kT} \frac{J^2}{\hbar^2 \omega_0} \left( \frac{\pi \sinh(\hbar\omega_0/2kT)}{\gamma} \right)^{1/2} e^{-2\gamma \tanh(\hbar\omega_0/4kT)}. \quad (1)$$

$a$  represents the spacing between molecular sites and  $J$  is the intermolecular resonance energy. Dispersion in the vibrational modes is neglected in Eq. (1) and the localized carrier is assumed to interact predominantly with phonons of energy  $\hbar\omega_0$ . The interaction parameter  $\gamma$  is defined by

$$\gamma = E_b / \hbar \omega_0,$$

where  $E_b$  denotes the polaron binding energy.

Equation (1) was derived for a one-dimensional model; in adapting it to the three-dimensional case a factor of the order of  $1/c$ , where  $c$  denotes the coordination number, should be included on the right-hand side of the equation.

In analyzing the experimental results by means of Eq. (1) it is obviously impossible to determine a unique set of parameters. Instead, Table II lists a range of the quantities  $E_b$ ,  $\hbar\omega_0$ , and  $J/c^{1/2}$ , such that a fit to the data can be obtained by suitable choice of the parameters within these limits. It should be stressed that such sets of  $E_b$ ,  $\hbar\omega_0$ , and  $J/c^{1/2}$  satisfy the rather stringent conditions given by Holstein for the applicability of Eq. (1).

Figure 8 shows examples of the fit to the experimental data for  $\beta\text{-N}_2$  using the sets of parameters indicated. It can be seen that curve (b) reproduces to some extent the flattening in the experimental curve at the higher temperature. de Wit<sup>23</sup> has calculated the temperature dependence of the hopping mobility on a model which includes 10% dispersion in the vibrational spectrum. Using the difference between de Wit's curves and the corresponding curves in the absence of dispersion, we attempted to estimate the effect of dispersion on the fit to our experimental data. It is concluded that 10% dispersion necessitates only small adjustments in the fitting parameters and certainly does not affect the ranges given in Table II. However, dispersion causes a more pronounced flattening of the  $\mu$ -vs- $1/T$  curves at higher temperatures and could therefore lead to a closer fit than curve (b) in Fig. 8.

TABLE II. Ranges of fitting parameters to the nonadiabatic hopping formula [Eq. (1)] for the  $\beta\text{-N}_2$  and  $\gamma\text{-O}_2$  results.

	$E_b$ (meV)	$\hbar\omega_0$ (meV)	$Jc^{-1/2}$ (meV)	$\gamma$
$\beta\text{-N}_2$	22-32	3.5-7.5	0.7-1.0	4-7
$\gamma\text{-O}_2$	40-65	3.5-8.5	3-6	7-14

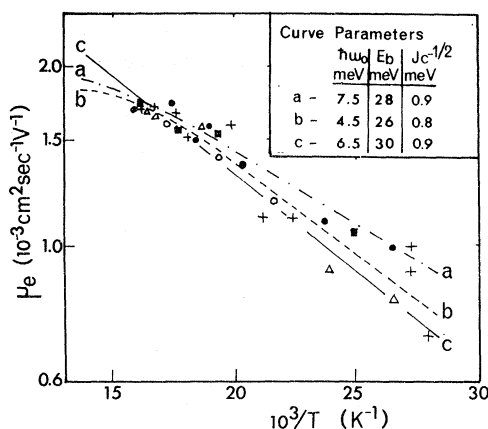


FIG. 8. Comparison of the temperature dependence of  $\mu_e$  calculated from Eq. (1) with the experimental data for  $\beta$  nitrogen (Fig. 3).

It was also tried to fit the results to alternative small-polaron models. In the adiabatic-hopping theory,<sup>24</sup> the required values for the phonon energy were unreasonably small. Munn and Siebrand's theory,<sup>25</sup> which includes a quadratic electron-phonon interaction, could not be fitted with feasible parameters which were at the same time consistent with the validity of the theory. Equation (1), on the other hand, based on the nonadiabatic model, led to consistent and reasonable parameters. With possible values of  $c$  between 2 and 12, an intermolecular resonance energy in the range from  $10^{-3}$  to  $10^{-2}$  eV is found, which is not unexpected for molecular crystals. However, the phonon energies in Table II appear at first sight surprisingly low, because intuitively one might have expected that the intramolecular stretching modes would predominate in the electron-phonon interaction. Clearly, this cannot be the case, because in diatomic solids such modes correspond to a phonon energy of about 200 meV.<sup>26</sup>

Siebrand<sup>26</sup> has discussed the effect of the vibrational interaction on bandwidth and carrier mobility in a number of diatomic crystals. He estimated  $E_b$  from spectroscopic data and then calculated  $\gamma$ , assuming that the predominant interaction occurred with the intramolecular stretching modes. On the basis of the present work this is incorrect, certainly for  $N_2$  and  $O_2$ , and it invalidates some of Siebrand's conclusions concerning Franck-Condon factors and bandwidths.

What is the nature of the low-energy vibrational modes? An interesting possibility is that the excess carriers in  $\beta$ - $N_2$  and  $\gamma$ - $O_2$  interact with the precessional modes of the molecules. Raman studies on  $\beta$ - $N_2$  and  $\gamma$ - $O_2$  show broad wings on the fundamental which extend to below  $100\text{ cm}^{-1}$ . The analysis of the  $\gamma$ - $O_2$  results<sup>7</sup> and of similar results

for the liquid phase<sup>27</sup> led to a broad frequency-distribution curve, which peaked at approximately  $50\text{ cm}^{-1}$ . This is consistent with the hindered rotation of the molecule, involving phonon energies of about 6 meV, very similar to those found from the transport measurements (Table II). However, it must be stressed that in spite of the numerical agreement, such an interpretation is by no means unique. Phonon energies associated with optical-lattice modes (only known for the  $\alpha$  phase of  $N_2$ <sup>28</sup>) are also of the same order of magnitude and interaction with the more energetic acoustic modes near the zone boundary cannot be excluded. The only definite conclusion that can be drawn at present is that molecular-stretching modes are not involved in the transport.

The results of Fig. 3 are an interesting example of the effect of the phase change on the electron mobility. It can be seen that  $\mu_e$  increases by a factor of three in going from the  $\beta$  to the  $\alpha$  phase. This could either be caused by a change in phonon energy (precessional modes do not exist in the  $\alpha$  phase) or by an increase in the resonance energy  $J$  between conducting states. Meaningful measurements of  $\mu_e(T)$  in the  $\alpha$  phase would help towards distinguishing between these possibilities.

Another problem concerns the molecular state of the localized carrier. If a single molecule only is involved, then the molecular-orbital picture suggests that the excess electron in  $N_2$  and the excess hole in  $O_2$  would both be in the  $1\pi^*$  state. However, it might be possible that the presence of the excess carrier results in the formation of a dimer state, such as  $O_4^+$ . This mechanism of localization has been suggested by Druger and Knox<sup>29</sup> for the excess holes in the rare-gas solids, and from our measurements<sup>10</sup> on Xe we would associate a binding energy  $1 < E_b < 50$  meV with the localized hole in a  $Xe_2^+$  center. The magnitude of  $E_b$  is not inconsistent with the calculation of Song<sup>30</sup> who obtained a value of  $E_b \sim 50$  meV for  $Ar_2^+$ . Unfortunately, similar calculations have not yet been performed for diatomic molecular solids; the similarity of the binding energies in Table II with the above values suggests that dimer localization may be a possibility.

Equation (1), used in the analysis of the results, is based on the assumption of uncorrelated hopping. Emin<sup>31</sup> has recently shown that if the dispersion of the vibrational modes is small, and consequently the lattice slow to relax after a hopping event, then the activation energy for the subsequent event could be appreciably smaller. In the case of  $N_2$ , Emin's condition for uncorrelated hopping becomes  $\mu \ll 3 \times 10^{-2}\text{ cm}^2\text{ sec}^{-1}\text{ V}^{-1}$ , if 10% dispersion is assumed. It seems, therefore, that correlation is unlikely to have much effect on the present results.

Finally, the orientational disorder which may arise from the molecular precession, could affect the  $E_b$  values deduced from the analysis. If, in a two-center model,  $W_D$  represents an energy difference in the quantized energy levels resulting from disorder, then in the high-temperature approximation to Eq. (1), the activation energy would be  $\frac{1}{2}(E_b + W_D)$ .<sup>32</sup> It is impossible to estimate  $W_D$  caused by the precessional motion with any certainty, and the  $E_b$  values in Table II have to be regarded with some caution.

## VI. CONCLUSIONS

(i) Electronic mobilities in the diatomic-molecular solids  $N_2$ ,  $O_2$ , and CO are low, lying between  $10^{-3}$  and  $10^{-2}$   $\text{cm}^2 \text{sec}^{-1} \text{V}^{-1}$  (Table I). In this respect diatomic solids differ basically from the rare-gas solids.

(ii) Transport is by phonon-assisted intermolecular hopping, and interpretation of the mobility

measurements in terms of the nonadiabatic small-polaron theory leads to consistent results, summarized in Table II.

(iii) Intramolecular stretching modes are not involved in the small-polaron transport. The low values of the deduced phonon energies suggest that excess carriers may interact with the precessional modes of the molecules, although other possibilities cannot be excluded.

(iv) Electronic transport was not observed in the corresponding molecular liquids. Positive and negative ions are mobile and Walden's rule is obeyed in each case. The step-wise changes in ionic mobility with applied field, first observed by Henson,<sup>17</sup> were not found in the present experiments.

## ACKNOWLEDGMENTS

One of us (R. J. L.) wishes to thank the Science Research Council and E. M. I. Ltd. for their financial assistance.

<sup>1</sup>D. C. Heberlein, E. D. Adams, and T. A. Scott, *J. Low-Temp. Phys.* **2**, 449 (1970).

<sup>2</sup>T. H. Jordan, H. W. Smith, W. E. Streib, and W. N. Lipscomb, *J. Chem. Phys.* **41**, 756 (1964).

<sup>3</sup>W. E. Streib, T. H. Jordan, and W. N. Lipscomb, *J. Chem. Phys.* **37**, 2962 (1962).

<sup>4</sup>A. S. De Reggi, P. C. Canepa, and T. A. Scott, *J. Magn. Resonance* **1**, 144 (1969).

<sup>5</sup>T. H. Jordan, W. E. Streib, H. W. Smith, and W. N. Lipscomb, *Acta Cryst.* **17**, 777 (1964).

<sup>6</sup>C. S. Barrett and L. Meyer, *Phys. Rev.* **160**, 694 (1967).

<sup>7</sup>J. E. Cahill and G. E. Leroi, *J. Chem. Phys.* **51**, 97 (1969).

<sup>8</sup>L. S. Miller, S. Howe, and W. E. Spear, *Phys. Rev.* **166**, 871 (1968).

<sup>9</sup>W. E. Spear and P. G. Le Comber, *Phys. Rev.* **178**, 1454 (1969).

<sup>10</sup>S. H. Howe, P. G. Le Comber, and W. E. Spear, *Solid State Commun.* **9**, 65 (1971).

<sup>11</sup>W. E. Spear, P. G. Le Comber, and R. J. Loveland (unpublished).

<sup>12</sup>Cryotip, supplied by Air Products and Chemicals Ltd.

<sup>13</sup>BOC grade-X gas. (a) Nitrogen (>99.999%); Ar <5 volume/10<sup>6</sup>; O<sub>2</sub>, H<sub>2</sub>, He, Ne, <1 volume/10<sup>6</sup>; CO<sub>2</sub>, hydrocarbons, <0.5 volume/10<sup>6</sup>. (b) Oxygen (>99.96%); Ar <100 volume/10<sup>6</sup>; H<sub>2</sub> <50 volume/10<sup>6</sup>; N<sub>2</sub> <10 volume/10<sup>6</sup>; CO<sub>2</sub>, CO, hydrocarbons <1 volume/10<sup>6</sup>. (c) Carbon monoxide (>99.95%); N<sub>2</sub> <400 volume/10<sup>6</sup>; CO<sub>2</sub> <100 volume/10<sup>6</sup>; H<sub>2</sub> <50 volume/10<sup>6</sup>; O<sub>2</sub> <20 volume/10<sup>6</sup>.

<sup>14</sup>CTAM/440 strips supplied by Getters (GB) Ltd.,

Croydon, England.

<sup>15</sup>W. E. Spear, *J. Non-Cryst. Solids* **1**, 197 (1969).

<sup>16</sup>W. Grevenconk, W. Herreman, and A. De Bock, *Physica* **46**, 600 (1970).

<sup>17</sup>B. L. Henson, *Phys. Rev.* **135**, A1002 (1964).

<sup>18</sup>L. Bruschi, G. Mazzi, and M. Santini, *Phys. Rev. Letters* **25**, 330 (1970).

<sup>19</sup>C. S. Doake and P. W. F. Gribbon, *J. Phys. A* **4**, 952 (1971).

<sup>20</sup>D. J. Gibbons and W. E. Spear, *J. Phys. Chem. Solids* **27**, 1917 (1966).

<sup>21</sup>T. Holstein, *Ann. Phys. (N. Y.)* **8**, 343 (1959).

<sup>22</sup>See, for instance, J. Appel, *Solid State Phys.* **21**, 26 (1968).

<sup>23</sup>H. J. de Wit, *Philips Res. Rept.* **23**, 449 (1968).

<sup>24</sup>D. Emin and T. Holstein, *Ann. Phys. (N. Y.)* **53**, 439 (1969).

<sup>25</sup>R. W. Munn and W. Siebrand, *J. Chem. Phys.* **52**, 6391 (1970).

<sup>26</sup>W. Siebrand, *J. Chem. Phys.* **41**, 3574 (1964).

<sup>27</sup>M. Blumenfeld, in *Molecular Dynamics and Structure of Solids*, edited by R. S. Carter *et al.*, Natl. Bur. Std. Special Publ. 301 (U. S. GPO, Washington, D. C., 1969), p. 441.

<sup>28</sup>A. Anderson, T. S. Sun, and M. C. A. Donkersloot, *Can. J. Phys.* **48**, 2265 (1970).

<sup>29</sup>S. D. Druger and R. S. Knox, *J. Chem. Phys.* **50**, 3142 (1969).

<sup>30</sup>K. Song, *Can. J. Phys.* **49**, 26 (1971).

<sup>31</sup>D. Emin, *Phys. Rev. Letters* **25**, 1751 (1970).

<sup>32</sup>J. Schnakenberg, *Phys. Status Solidi* **28**, 623 (1968).